Revealing Different Aggregation Pathways of Amyloidogenic Proteins by Ultrasound Velocimetry

Vytautas Smirnovas and Roland Winter
University of Dortmund, Department of Chemistry, Physical Chemistry I, Biophysical Chemistry, Dortmund, Germany

ABSTRACT In this work, we performed a detailed thermodynamic study, including ultrasound velocimetry, densimetry, calorimetry, and FTIR spectroscopy, of an aggregation-prone protein (insulin) under different salt-screening conditions to gain a deeper insight into the scenario of physicochemical events during its temperature-induced unfolding and aggregation reactions. Differences in aggregation and fibrillization pathways are reflected in changes of the partial molar volume, the coefficients of thermal expansion and compressibility, and the infrared spectral properties of the protein. Combining all experimental data allows setting up a scheme for the temperature-dependent insulin aggregation reaction in the presence and absence of NaCl. As revealed by complementary atomic force microscopy studies, under charge-screening conditions, a process involving structural reorganization, ripening, and formation of more compact nuclei from amorphous oligomers is involved in the formation of mature fibrillar morphologies. In this work, our focus was to put forward a comprehensive discussion of the use of ultrasound velocimetry in disentangling different aggregation pathways. In fact, ultrasound velocimetry proved to be very sensitive to changes in aggregation pathway, highlighting the importance of density and compressibility changes in the different aggregation and fibrillization reactions of the protein.

INTRODUCTION

Since the formation of orderly aggregated proteins was found to be associated with several neurodegenerative disorders, such as Alzheimer's, Creutzfeldt-Jakob's, and Parkinson's disease, the problem of protein aggregation has begun to receive considerable attention (1–3). Although the physics underlying this process remains poorly understood, a growing body of evidence suggests that formation of linearly ordered protein aggregates, the so-called amyloids, is a common, generic feature of proteins as polymers (1). Protein aggregation is also of considerable interest in the pharmaceutical industry, where maintaining the stability of proteins is vital during the production, purification, and long-term storage of protein-based drugs such as insulin. From the thermodynamic point of view, the partial protein volume and its temperature and pressure derivatives, as well as enthalpy and volume fluctuations, are the parameters determining protein stability, unfolding, and aggregation behavior. These parameters can be monitored by differential scanning calorimetry (DSC), pressure perturbation calorimetry, densimetry, and ultrasound velocimetry (4–9). Through such a combination of methods, one obtains a detailed thermodynamic description of proteins, linking the thermodynamics to the generic behavior of protein aggregation. In recent years, it has also become clear that different solvation, temperature, and pressure conditions may lead to different aggregation pathways and fibril morphologies (10–12).

In this work, we put forward a comprehensive discussion of the use of ultrasound velocimetry in disentangling different aggregation pathways. As a case study, we present data on insulin aggregation and fibrillization under conditions without and with 0.1 M NaCl. Insulin is a common model protein for studies on amyloidogenesis, which easily forms amyloidlike fibrils with β-pleated sheet structure and distinct staining properties under denaturing conditions, such as high temperature and low pH (13–21, and references therein). The aggregation-competent intermediate, a partly unfolded monomer, which is formed upon an endothermic transition, is thought to undergo subsequently exothermic intermolecular stacking, leading to aggregation, fibrillization of the aggregate, and simultaneous release of solvational water, as suggested in our recent DSC and pressure perturbation calorimetry studies (19).

MATERIALS AND METHODS

Bovine pancreatic insulin was purchased from Sigma Aldrich (Munich, Germany). Density measurements were carried out with a DMA 5000 vibrating tube densimeter with a precision of $\pm 5 \times 10^{-6}$ g cm^{-3}. The temperature was increased in a stepwise manner from 25 to 85°C at an average heating rate of 20°C h^{-1}. The partial specific volume of the protein was calculated using

$$v^{o} = \frac{1}{c} - \frac{\rho - c}{\rho_0 c}, \quad (1)$$

where ρ and ρ_0 are the densities of the solution and solvent, respectively, and c is the specific concentration of the protein (8).

The ultrasonic measurements were carried out using an ultrasonic resonator device (ResoScan system, TF Instruments, Heidelberg, Germany) with ultrasonic transducers made of single crystal lithium niobate of a fundamental frequency of 9.5 MHz. The instrument comprises two independent cells with a path length of 7.0 mm for sample and reference. They are

Submitted October 1, 2007, and accepted for publication December 11, 2007.

Address reprint requests to Roland Winter, Dept. of Chemistry, Physical Chemistry I, Biophysical Chemistry, University of Dortmund, Otto-Hahn Straße 6, D-44227 Dortmund, Germany. Tel.: 49-231-755-3900; Fax: 49-231-755-3901; E-mail: roland.winter@uni-dortmund.de.

Editor: Heinrich Roder.

0006-3495/08/04/3241/06 $2.00

doi: 10.1529/biophysj.107.123133

embedded into a metal-block Peltier thermostat with a temperature stability of ±0.001°C. The resolution of the ultrasonic velocity measurements is 0.001 m s^{-1}. Ultrasonic velocities of insulin samples (U) and buffer (U_0) were measured over the same temperature range and at the same heating rate (20°C h^{-1}).

DSC measurements were carried out on a VP DSC calorimeter from MicroCal (Northampton, MA). The calorimeter's sample cell was filled with ~0.5 mL of solution, whereas the reference cell was filled with a matching buffer. Measurements were carried out from 25 to 85°C at a heating rate of 20°C h^{-1}.

The FTIR spectra were recorded using a Nicolet 5700 spectrometer from Thermo Scientific (Waltham, MA) equipped with a liquid-nitrogen-cooled mercury-cadmium-telluride detector. A 2% (w/w) solution of insulin in D_2O (instead of H_2O, to avoid overlap with the amide I band region) with and without 0.1 M NaCl, was adjusted to pH 2 using DCl. For all measurements, CaF_2 transmission windows and 0.05 mm Mylar spacers were used (19). Temperature was increased in a stepwise manner from 25 to 85°C at an average heating rate of 20°C h^{-1}. For each spectrum, 256 interferograms of 2 cm^{-1} resolution were co-added. From the spectrum of each sample at each temperature, a corresponding buffer spectrum was subtracted. All the spectra were baseline-corrected and normalized before further data processing. The progress of the α-helix-to-β-sheet transition upon aggregation was quantified as $(I - I_i)/(I_f - I_i)$, where I_i is the initial spectral intensity at 1627 cm^{-1} of the native insulin (first spectrum), I_f is the final intensity after aggregation is complete, and I is the transient intensity at this wavenumber. All data processing was performed with GRAMS software (Thermo Scientific).

To be able to compare all the physical parameters measured by these different techniques, the same heating rate was used in all experiments (20°C h^{-1}), because above ~60°C, kinetic phenomena also are involved (12).

RESULTS AND DISCUSSION

Fig. 1 shows FTIR spectra of 2 wt % insulin at 25, 65, and 85°C in the absence and presence of salt. Above 60°C, insulin is known to partially unfold and aggregate (19). At 25°C, in the native folded state, the spectra exhibit maxima in the amide I′ band region at ~1653 cm^{-1} (minima of second derivative at 1656 cm^{-1}), which is typical for insulin's predominantly α-helical structure. The spectra obtained at 85°C, when the protein has undergone unfolding and subsequent aggregation and fibrillization, also do not differ markedly for the two solutions of different ionic strength. They show maxima at 1628 cm^{-1} (with the main minimum of the second derivative at 1628 cm^{-1} and a weaker one at 1619 cm^{-1}) in the presence of 0.1 M NaCl, and a slightly broader peak at 1627 cm^{-1} (main minimum of second derivative at 1628 cm^{-1} and a weaker one at 1618 cm^{-1}) in the absence of salt. Both cases are typical for formation of parallel intermolecular β-sheet-rich secondary structures (19).

The main difference between the two sample conditions is hidden in the intermediate temperature range. In the absence of NaCl, the FTIR spectrum at 65°C shows a broad maximum at 1648 cm^{-1}, which indicates significant unfolding of the protein to a random secondary structure. Conversely, in the presence of salt, i.e., under charge-screening conditions, we envisage a completely different picture: a broad β-sheet peak appears, with a maximum between 1620 and 1628 cm^{-1} (main minimum of the second derivative at 1619 cm^{-1} and a weaker one at 1628 cm^{-1}) and a broad shoulder around 1646 cm^{-1}, characteristic of disordered secondary structures. The β-sheet spectrum at 65°C in the presence of 0.1 M NaCl can be assigned to formation of nonfibrillar aggregates (or oligomers), as seen in AFM images (see below, Fig. 4 *A*, and (12)), and both spectra at 85°C represent mature amyloid fibrils.

Further processing of the FTIR data allowed calculation of the evolution of β-sheet-rich structures with increasing temperature. The different regions seen in Fig. 2 *A* for the

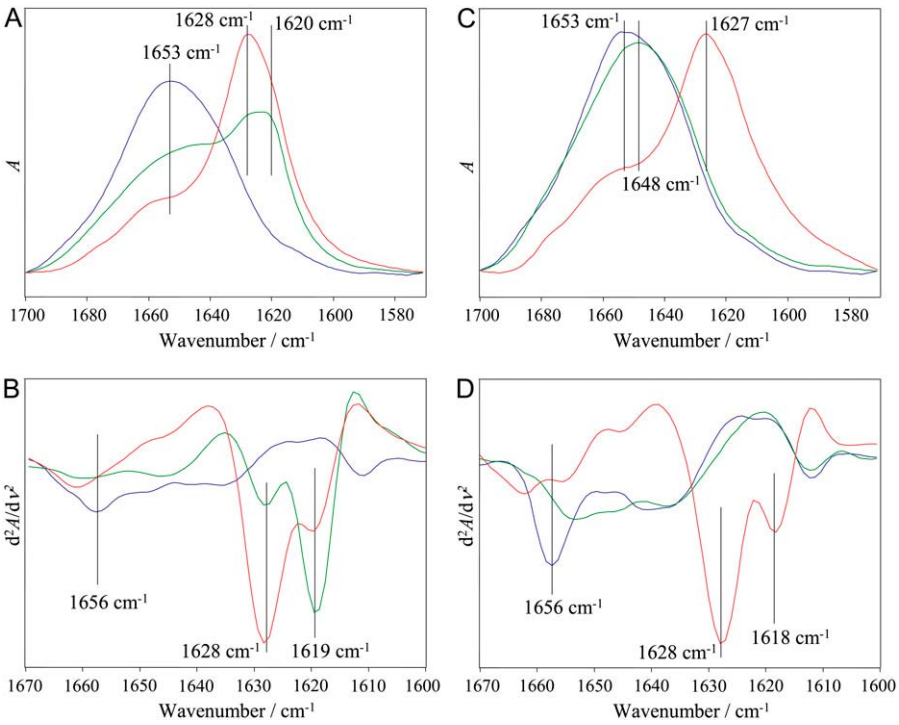

FIGURE 1 (*A* and *C*) Amide I/I′ band region of FTIR spectra of 2% insulin in D_2O, pH 2, in the presence (*A*) and absence (*C*) of 0.1 M NaCl at three selected temperatures. (*B* and *D*) Second derivatives of the spectra in *A* and *B*, which allow for a more accurate analysis of band maxima. *Blue lines*, $T = 25$°C; *green lines*, $T = 65$°C; and *red lines*, $T = 85$°C.

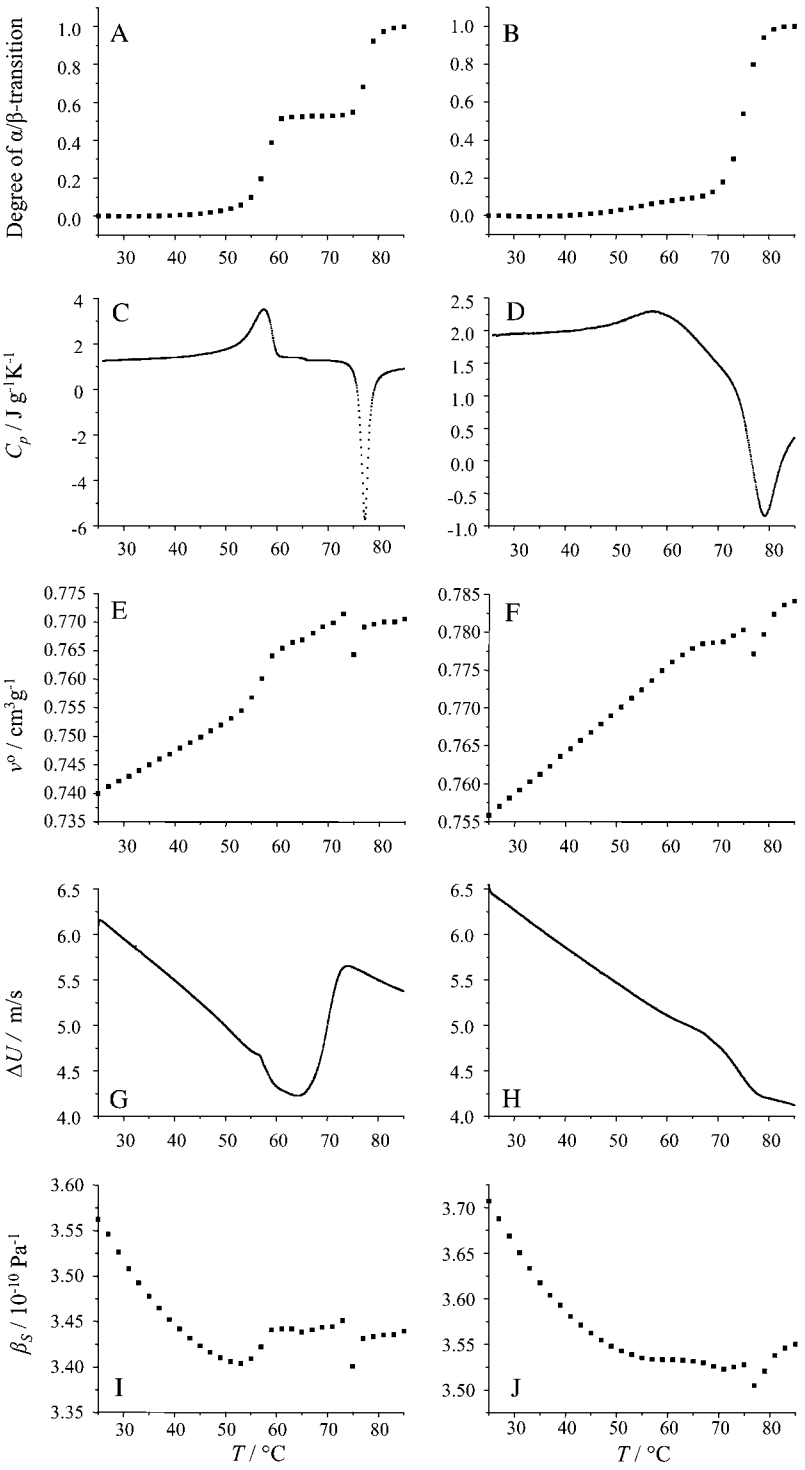

FIGURE 2 Degree of α-to-β transition as derived from the FTIR spectra (*A* and *B*), the measured specific heat capacity (*C* and *D*), partial specific protein volume (*E* and *F*), sound velocity difference (*G* and *H*), and adiabatic compressibility coefficient (*I* and *J*) in the presence (*left column*) and absence (*right column*) of 0.1 M NaCl.

sample in the presence of NaCl represent the formation of early (amorphous) aggregate species, which takes place between 55 and 60°C, their persistence between 60 and 75°C, and the formation of mature fibrils between 75 and 80°C. Fig. 2 *B* shows the corresponding data for aggregating insulin in salt-free solution. In this case, we observe no significant change in β-sheet content between 55 and 70°C, except that H-D exchange (amide II band region) and broadening of the amide I′ band take place due to partial unfolding of the protein; this is followed by formation of fibrils between 70 and 80°C.

The DSC measurements exhibit an endothermic peak in the preaggregated regime between 50 and 60°C for the 0.1 M NaCl solution (Fig. 2 *C*) and a broad peak due to partial

unfolding between 50 and 70°C for the salt-free solution (Fig. 2 *D*). Further unfolding and subsequent fibril formation (sharp exothermic peaks) appear between 75 and 80°C (Fig. 2 *C*) and 70 and 85°C (Fig. 2 *D*) for the NaCl and salt-free solutions, respectively.

The corresponding data of the partial specific volume, v^o, and sound velocity, U, are shown in Fig. 2, *E–H*. From measurements of v^o and U, the partial molar compressibility, K_S^o, can be determined using the Newton-Laplace equation, which relates the coefficient of adiabatic compressibility of a medium,

$$\beta_S = -\frac{1}{V}\left(\frac{\partial V}{\partial p}\right)_S, \tag{2}$$

with its density, ρ, and sound velocity, U:

$$U^2 = (\beta_S \rho)^{-1}, \tag{3}$$

where $K_S^o = V^o\beta_S$ (6–8). For dilute solutions,

$$K_S^o = \beta_{S0}\left(2V^o - 2[U] - \frac{M}{\rho_0}\right), \tag{4}$$

where the partial molar volume of the protein $V^o = (\partial V/\partial n)_{T,p}$, M is its molar mass, the relative molar sound velocity (increment) of the solute $[U] = (U - U_0)/(U_0 \times C)$; U and U_0 are the sound velocities of the solute and solvent, respectively; and C is the molar concentration of the protein.

Experimental data on the coefficient of isothermal compressibility, $\beta_T = K_T^o/V^o$, of proteins are very scarce, as it is technically challenging to measure the partial volume as a function of the pressure using densimetric techniques with high precision (22). However, the partial molar isothermal compressibility of the solute can be obtained from the adiabatic value by

$$K_T^o = K_S^o + \left(\frac{T\alpha_0^2}{\rho_0 c_{p0}}\right)\left(\frac{2E^o}{\alpha_0} - \frac{C_p^o}{\rho_0 c_{p0}}\right), \tag{5}$$

where c_{p0} is the specific heat capacity at constant pressure of the solvent, α_0 is the coefficient of thermal expansion of the solvent, and $E^o = (\partial V^o/\partial T)_p$ is the partial molar expansibility of the solute (7,8). C_p^o is the partial molar heat capacity of the solute, and T is the absolute temperature. The specific heat capacity of the protein at constant pressure has been obtained from

$$c_p = \frac{\Delta C_p}{m} + \frac{v^o c_{p0}}{v_0^o}, \tag{6}$$

ΔC_p is the heat capacity difference between the sample solution and solvent reference cell as obtained by the DSC calorimeter; v^o and v_0^o are the partial specific volumes of the solute and solvent, respectively. The coefficient of the isothermal compressibility, β_T, allows calculation of the volume fluctuations of a system using the expression $\langle(\Delta V)^2\rangle = k_B T V \beta_T$. This equation cannot be directly used for partial molar volume or compressibility data, as these still contain significant (even negative) hydration contributions from the first water layers hydrating the protein. However, qualitative conclusions can still be drawn.

Formation of nonfibrillar aggregates (in the presence of NaCl) leads to a decrease of the sound velocity with respect to the solvent (see Fig. 2 *G*) and is accompanied by an increase of the partial specific volume (Fig. 2 *E*), hence resulting in a positive change in partial adiabatic compressibility; β_S increases from 3.4×10^{-10} Pa^{-1} at 53°C to 3.44×10^{-10} Pa^{-1} at 59°C (Fig. 2 *I*). The corresponding isothermal compressibility, which is proportional to the volume fluctuations of the system, increases by ~7% in this temperature regime; β_T increases from 3.75×10^{-10} Pa^{-1} at 25°C to 5.2×10^{-10} Pa^{-1} at 59°C. As these early aggregate structures occupy a ~1% larger partial specific volume compared to the native protein, application of pressure should be able to retard formation of such species, leading to dissociation, as has in fact been observed recently (12). Subsequent formation of elongated fibrils leads to a decrease of the partial specific volume and an increase in sound velocity and, hence, a negative change in partial adiabatic compressibility. Different from the amorphous aggregates, the tight packing of β-sheets and depletion of internal cavities in the late fibrillar aggregates leads to a compaction and hence ~1% reduction of the final value of the partial specific protein volume. The decrease in solvent-accessible area is also reflected in a negative change of C_p (Fig. 2, *C* and *D*).

Conversely, for the salt-free insulin solution, only a minor increase in the sound velocity is observed between 65 and 70°C (Fig. 2 *H*), which is accompanied by a small decrease in partial specific volume (Fig. 2 *F*), and a small decrease of the partial adiabatic (0.3%) and isothermal compressibility (0.9%), as is typical for significant unfolding of proteins (7). When the final mature fibrils are formed, the sound speed remains small, which is due to a slight increase in β_S.

By comparison of the data sets for both samples (with and without NaCl), we notice that most of the differences in the mechanism of aggregation occur in the intermediate temperature range where nucleation and growth take place. On the one hand (in the presence of screening salt solution), formation of long-lived oligomeric precursors and nonfibrillar aggregates is observed. On the other hand, in the absence of salt, further unfolding of the monomer and formation of elongated fibrillar structures occurs. The FTIR data suggest a common secondary structure of the final fibrils, however. The DSC data reveal that both aggregation processes are strongly exothermic (with the difference of a broader peak in the absence of NaCl, which could be due to the slower process itself). A marked decrease of the partial specific volume at the onset of fibril formation, which is followed by an increase during the further aggregation reaction, is visible in both samples. Such behavior may be explained by the (partial) unfolding of the protein initiating the process, which is connected with a release of void volume and electrostrictive

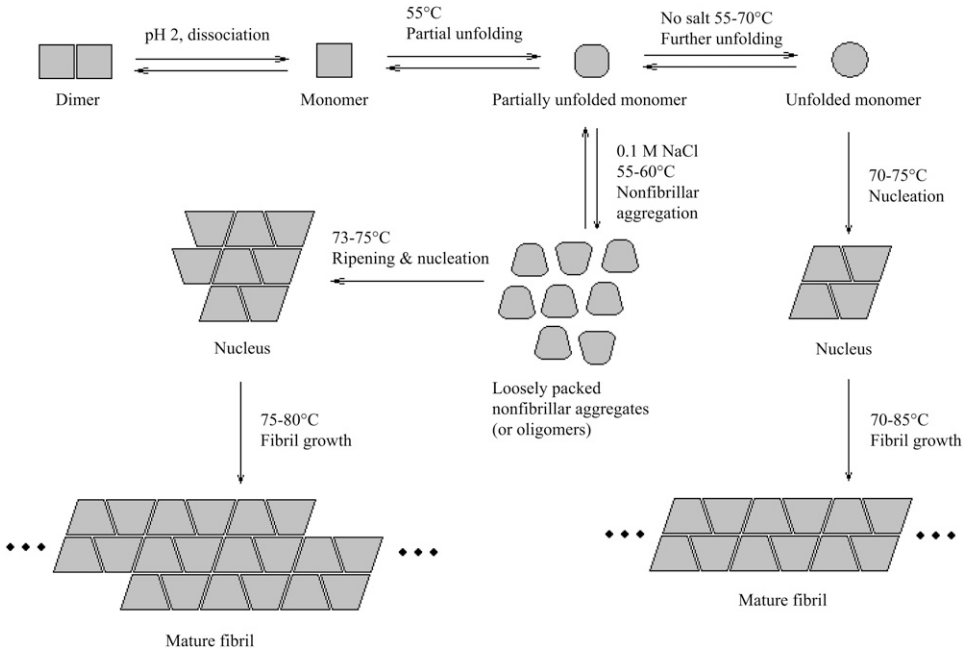

FIGURE 3 Proposed scheme for the temperature-dependent insulin aggregation pathways in the presence and absence of salt (0.1 M NaCl).

hydration, as well as formation of densely packed nuclei. This is followed by elongation of fibrils, which leads to a smaller water-accessible surface area and, hence, a small increase of partial volume due to a decreased hydration.

In fact, ultrasound velocimetry, which depends on changes in density and compressibility, appears to be the technique most sensitively able to reveal differences in the mechanism of the aggregation and fibrillation reaction. Combining the data from FTIR spectroscopy, ultrasound velocimetry, densimetry, and DSC makes it possible to set up a scheme for the temperature-dependent insulin aggregation reaction in the presence and absence of 0.1 M NaCl (Fig. 3). In the absence of screening salt, with increasing temperature insulin starts to destabilize and unfold, and, after reaching a significant level of unfolding (random-coil secondary structures are dominating), forms compact nuclei that grow into fibrils. In the presence of 0.1 M NaCl, partial unfolding (the contents of disordered, random-coil secondary structures is below 50%) occurs with rising temperature, forming partially unfolded nonfibrillar aggregates (or oligomers) around 55–60°C. Further increase of temperature leads to a reorganization of the aggregate structure and formation of more compact nuclei, which allows growth of elongated mature fibrillar species. As revealed by AFM (Fig. 4), the latter process, which implements structural reorganization, ripening, and formation of more compact nuclei from amorphous oligomers, leads to formation of more crowded and larger aggregate morphology (entangled networks, floccules).

Besides the changes in ionic strength, shown in this work, cosolvents and the application of pressure have also proved to be valuable parameters to tune nucleation and growth processes and to elucidate novel aggregation pathways of amyloidogenic proteins, which may lead to different aggregate morphologies (23–31). In the case of the pressure variable, aggregation pathways and morphologies are selected that can be controlled by minimizing the system volume, whereas in the case of salts, cosolvents, and temperature, solvational effects and activation energies largely determine the kinetics of the aggregation and fibrillation process.

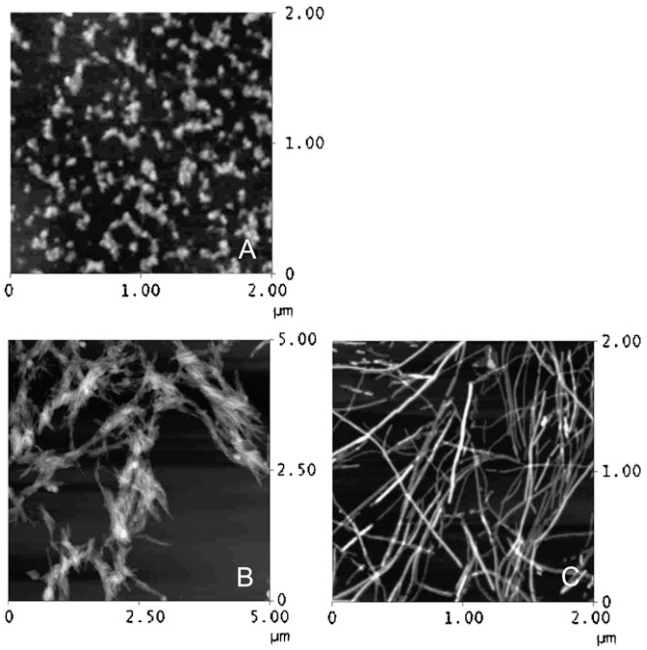

FIGURE 4 AFM pictures of nonfibrillar aggregates formed in the presence of 0.1 M NaCl (*A*), and typical mature insulin amyloid fibrils formed in the presence (*B*) or absence (*C*) of 0.1 M NaCl. In the absence of NaCl, ordinary fibrils of 4–8 nm diameter are formed, whereas in the presence of NaCl, part of the fibrils stick together, forming large aggregates up to 100 nm in height. The nonfibrillar aggregates vary in height from 0.5 to 1.5 nm.

Financial support from the Deutsche Forschungsgemeinschaft, the country Nordrhein-Westfalen, and the European Union (Europäischer Fonds für regionale Entwicklung) is gratefully acknowledged.

REFERENCES

1. Chiti, F., and C. M. Dobson. 2006. Protein misfolding, functional amyloid, and human disease. *Annu. Rev. Biochem.* 75:333–366.
2. Kelly, J. W. 1998. The alternative conformations of amyloidogenic proteins and their multi-step assembly pathway. *Curr. Opin. Struct. Biol.* 8:101–106.
3. Lansbury, P. T., and H. A. Lashuel. 2006. A century-old debate on protein aggregation and neurodegeneration enters the clinic. *Nature.* 443:774–779.
4. Heerklotz, H. 2004. The microcalorimetry of lipid membranes. *J. Phys. Condens. Matter.* 16:R441–R467.
5. Mitra, L., N. Smolin, R. Ravindra, C. Royer, and R. Winter. 2006. Pressure perturbation calorimetric studies of the solvation properties and the thermal unfolding of proteins in solution: experiments and theoretical interpretation. *Phys. Chem. Chem. Phys.* 8:1249–1265.
6. Gekko, K., and Y. Hasegawa. 1989. Effect of temperature on the compressibility of native globular proteins. *J. Phys. Chem.* 93:426–429.
7. Chalikian, T. V. 2003. Volumetric properties of proteins. *Annu. Rev. Biophys. Biomol. Struct.* 32:207–235.
8. Smirnovas, V., R. Winter, T. Funck, and W. Dzwolak. 2005. Thermodynamic properties underlying the α-helix-to-β-sheet transition, aggregation and amyloidogenesis of polylysine as probed by calorimetry, densimetry and ultrasound velocimetry. *J. Phys. Chem. B.* 109:19043–19045.
9. Smirnovas, V., R. Winter, T. Funck, and W. Dzwolak. 2006. Protein amyloidogenesis in the context of volume fluctuations: a case study on insulin. *ChemPhysChem.* 7:1046–1049.
10. Søndergaard Pedersen, J., J. M. Flink, D. Dikov, and D. E. Otzen. 2006. Sulfates dramatically stabilize a salt-dependent type of glucagon fibrils. *Biophys. J.* 90:4181–4194.
11. Petkova, A. T., R. D. Leapman, Z. Guo, W.-M. Yau, M. P. Mattson, and R. Tycko. 2005. Self-propagating, molecular-level polymorphism in Alzheimer's β-amyloid fibrils. *Science.* 307:262–265.
12. Grudzielanek, S., V. Smirnovas, and R. Winter. 2006. Solvation-assisted pressure tuning of insulin fibrillation: from novel aggregation pathways to biotechnological applications. *J. Mol. Biol.* 356:497–509.
13. Jimenez, J. L., E. J. Nettleton, M. Bouchard, C. V. Robinson, C. M. Dobson, and H. R. Saibil. 2002. The protofilament structure of insulin amyloid fibrils. *Proc. Natl. Acad. Sci. USA.* 99:9196–9201.
14. Mauro, M., E. F. Craparo, A. Podestà, D. Bulone, R. Carrotta, V. Martorana, G. Tiana, and P. L. San Biagio. 2007. Kinetics of different processes in human insulin amyloid formation. *J. Mol. Biol.* 366:258–274.
15. Ahmad, A., I. S. Millett, S. Doniach, V. N. Uversky, and A. L. Fink. 2003. Partially folded intermediates in insulin fibrillation. *Biochemistry.* 42:11404–11416.
16. Dzwolak, W., V. Smirnovas, R. Jansen, and R. Winter. 2004. Insulin forms amyloid in a strain-dependent manner: an FT-IR spectroscopy study. *Protein Sci.* 13:1927–1932.
17. Dzwolak, W., A. Loksztejn, and V. Smirnovas. 2006. New insights into the self-assembly of insulin amyloid fibrils: an H-D exchange FT-IR study. *Biochemistry.* 45:8143–8151.
18. Dzwolak, W., R. Ravindra, and R. Winter. 2004. Hydration and structure: the two sides of the insulin aggregation process. *Phys. Chem. Chem. Phys.* 6:1938–1943.
19. Dzwolak, W., R. Ravindra, J. Lendermann, and R. Winter. 2003. Aggregation of bovine insulin probed by DSC/PPC calorimetry and FTIR spectroscopy. *Biochemistry.* 42:11347–11355.
20. Jansen, R., W. Dzwolak, and R. Winter. 2005. Amyloidogenic self-assembly of insulin aggregates probed by high resolution atomic force microscopy. *Biophys. J.* 88:1344–1353.
21. Smith, M. I., J. S. Sharp, and C. J. Roberts. 2007. Nucleation and growth of insulin fibrils in bulk solution and at hydrophobic polystyrene surfaces. *Biophys. J.* 93:2143–2151.
22. Seemann, H., R. Winter, and C. A. Royer. 2001. Volume, expansivity and isothermal compressibility changes associated with temperature and pressure unfolding of staphylococcal nuclease. *J. Mol. Biol.* 307:1091–1102.
23. Cordeiro, Y., J. Kraineva, M. P. Gomes, M. H. Lopes, V. R. Martins, L. M. Lima, D. Foguel, R. Winter, and J. L. Silva. 2005. The amino-terminal PrP domain is crucial to modulate prion misfolding and aggregation. *Biophys. J.* 89:2667–2676.
24. Dzwolak, W., S. Grudzielanek, V. Smirnovas, R. Ravindra, C. Nicolini, R. Jansen, A. Loksztejn, S. Porowski, and R. Winter. 2005. Ethanol-perturbed amyloidogenic self-assembly of insulin: looking for origins of amyloid strains. *Biochemistry.* 44:8948–8958.
25. Jansen, R., S. Grudzielanek, W. Dzwolak, and R. Winter. 2004. High pressure promotes circularly shaped insulin amyloid. *J. Mol. Biol.* 338: 203–206.
26. Grudzielanek, S., R. Jansen, and R. Winter. 2005. Solvational tuning of the unfolding, aggregation and amyloidogenesis of insulin. *J. Mol. Biol.* 351:879–894.
27. Cordeiro, Y., J. Kraineva, R. Ravindra, L. M. Lima, M. P. Gomes, D. Foguel, R. Winter, and J. L. Silva. 2004. Hydration and packing effects on prion folding and β-sheet conversion. High pressure spectroscopy and pressure perturbation calorimetry studies. *J. Biol. Chem.* 279:32354–32359.
28. Foguel, D., M. C. Suarez, A. D. Ferrão-Gonzales, T. C. Porto, L. Palmieri, C. M. Einsiedler, L. R. Andrade, H. A. Lashuel, P. T. Lansbury, J. W. Kelly, and J. L. Silva. 2003. Dissociation of amyloid fibrils of α-synuclein and transthyretin by pressure reveals their reversible nature and the formation of water-excluded cavities. *Proc. Natl. Acad. Sci. USA.* 100:9831–9836.
29. Niraula, T. N., T. Konno, H. Li, H. Yamada, K. Akasaka, and H. Tachibana. 2004. Pressure-dissociable reversible assembly of intrinsically denatured lysozyme is a precursor for amyloid fibrils. *Proc. Natl. Acad. Sci. USA.* 101:4089–4093.
30. Foguel, D., and J. L. Silva. 2004. New insights into the mechanisms of protein misfolding and aggregation in amyloidogenic diseases derived from pressure studies. *Biochemistry.* 43:11361–11370.
31. St. John, R. J., J. F. Carpenter, and T. W. Randolph. 1999. High pressure fosters protein refolding from aggregates at high concentrations. *Proc. Natl. Acad. Sci. USA.* 96:13029–13033.